

Supplemental Materials

Toxicological Profiling of Metal Oxide Nanoparticles in Liver Context reveals Pyroptosis in Kupffer Cells and Macrophages *Versus* Apoptosis in Hepatocytes

*Vahid Mirshafiee,^{†, ‡, #} Bingbing Sun,^{‡, #} Chong Hyun Chang,[†] Yu-Pei Liao,[‡] Wen Jiang,[†]
Jinhong Jiang,[†] Xiangsheng Liu,[‡] Xiang Wang,[†] Tian Xia,^{†, ‡, *} and André E. Nel^{†, ‡, *}*

[†]Center for Environmental Implications of Nanotechnology, California NanoSystems Institute, University of California Los Angeles, 570 Westwood Plaza, Los Angeles, California 90095, United States

[‡]Division of NanoMedicine, Department of Medicine, University of California Los Angeles, 10833 Le Conte Ave., Los Angeles, California 90095, United States

[‡]State Key Laboratory of Fine Chemicals, Department of Chemical Engineering, Dalian University of Technology, 2 Linggong Rd., Dalian 116024, China

* Address correspondence to:

txia@ucla.edu

anel@mednet.ucla.edu

[#]These authors contributed equally to this work

Table S1. MOx nanoparticle library, depicting the commercial source, crystal structure, primary size, hydrodynamic size and zeta potential. The hydrodynamic size and zeta potential were determined in deionized water and complete cell culture medium (supplemented with 10% fetal bovine serum). While some of the data for primary particle size and crystallinity were obtained from our historical data bank (see previous publications as listed below the table), new measurements were obtained for newly introduced REOs.

Nanoparticles	Source	Crystal Structure	Primary Size (nm)	Hydrodynamic Size (nm)		z-Potential (mV)	
				DI Water	DMEM	DI Water	DMEM
Al ₂ O ₃	Meliorum	Rhombohedral*	14.7 ± 5.2*	441.4 ± 22.4	428.4 ± 6.2	41.0 ± 0.7	-12.0 ± 1.0
CeO ₂	Meliorum	Cubic*	18.3 ± 6.8*	541.9 ± 27.1	250.3 ± 3.2	21.9 ± 0.8	-15.3 ± 0.7
CoO	US-Nano	Cubic*	71.8 ± 16.2*	830.1 ± 38.4	585.6 ± 16.4	23.2 ± 1.9	-12.8 ± 1.5
Co ₃ O ₄	Lutz Madler	Cubic*	10.0 ± 2.4*	336.7 ± 5.5	311.7 ± 3.7	23.9 ± 2.1	-10.7 ± 1.2
Cr ₂ O ₃	US-Nano	Rhombohedral*	193.0 ± 90.0*	284.7 ± 3.7	298.8 ± 2.2	-17.9 ± 0.3	-9.5 ± 1.8
CuO	Lutz Madler	Monoclinic*	12.8 ± 3.4*	266.0 ± 9.8	284.7 ± 5.2	26.8 ± 1.5	-12.2 ± 1.0
Dy ₂ O ₃	US-Nano	Cubic	37.5 ± 6.6*	818.4 ± 37.9	738.6 ± 40.1	9.7 ± 1.6	-9.1 ± 0.6
Er ₂ O ₃	US-Nano	Cubic	113.8 ± 37.8*	390.6 ± 19.7	267.4 ± 3.6	34.0 ± 1.4	-16.4 ± 3.1
Eu ₂ O ₃	US-Nano	Cubic	52.8 ± 11.7*	379.5 ± 7.3	588.1 ± 11.9	31.8 ± 1.2	-14.9 ± 1.8
Fe ₂ O ₃	US-Nano	Rhombohedral*	12.3 ± 2.9*	296.5 ± 12.8	377.8 ± 15.9	20.7 ± 2.2	-15.2 ± 3.5
Fe ₃ O ₄	Lutz Madler	Cubic*	12.0 ± 3.2*	146.2 ± 1.6	218.4 ± 3.4	-23.6 ± 0.2	-14.2 ± 2.2
Gd ₂ O ₃	NanoAmor	Cubic*	43.8 ± 15.8*	655.3 ± 16.5	898.0 ± 13.2	34.6 ± 2.3	-10.7 ± 1.4
HfO ₂	US-Nano	Monoclinic*	28.4 ± 7.3*	369.7 ± 3.1	237.8 ± 7.6	26.3 ± 1.4	-12.6 ± 2.2
In ₂ O ₃	US-Nano	Cubic*	59.6 ± 19.0*	193.4 ± 5.4	241.8 ± 5.2	50.1 ± 1.4	-13.6 ± 2.7
La ₂ O ₃	NanoAmor	Hexagonal*	24.6 ± 5.3*	997.1 ± 98.6	874.3 ± 32.8	13.4 ± 1.1	-11.3 ± 0.7
Mn ₂ O ₃	NanoAmor	Tetragonal*	51.5 ± 7.3*	493.0 ± 21.4	426.7 ± 18.9	-48.5 ± 0.6	-14.0 ± 1.1
Nd ₂ O ₃	NanoAmor	Cubic	133.8 ± 51.6*	448.4 ± 13.6	338.8 ± 3.2	18.5 ± 0.3	-14.6 ± 1.7
NiO	Sigma	Cubic*	13.1 ± 5.9*	425.6 ± 6.4	457.4 ± 3.0	43.0 ± 0.2	-12.8 ± 2.9
Ni ₂ O ₃	US-Nano	Hexagonal*	140.6 ± 52.5*	482.8 ± 14.7	339.6 ± 12.9	18.5 ± 1.1	-11.3 ± 1.7
Sb ₂ O ₃	Lutz Madler	Orthorhombic*	11.8 ± 3.3*	237.4 ± 16.4	235.2 ± 5.0	-34.6 ± 1.0	-13.6 ± 3.3
SiO ₂	NanoAmor	N/A*	13.5 ± 4.2*	337.8 ± 20.8	277.2 ± 8.5	-37.3 ± 1.5	-15.4 ± 4.0
Sm ₂ O ₃	US-Nano	Cubic	108.3 ± 47.4*	797.3 ± 57.0	797.6 ± 14.7	40.1 ± 1.8	-11.4 ± 2.6
SnO ₂	US-Nano	Tetragonal*	62.4 ± 13.2*	493.3 ± 23.6	538.1 ± 13.4	-38.6 ± 0.6	-13.5 ± 0.9
TiO ₂	Lutz Madler	Tetragonal*	12.6 ± 4.3*	229.5 ± 5.4	201.9 ± 3.5	4.0 ± 0.4	-11.9 ± 1.6
WO ₃	Lutz Madler	Monoclinic*	16.6 ± 4.3*	119.1 ± 4.5	116.2 ± 8.4	-44.9 ± 1.3	-14.5 ± 1.8
Y ₂ O ₃	Meliorum	Cubic*	32.7 ± 8.1*	1004.1 ± 166.8	500.1 ± 33.0	28.5 ± 1.6	-9.8 ± 1.1
Yb ₂ O ₃	MK-Nano	Cubic*	61.7 ± 11.3*	601.8 ± 29.6	352.8 ± 53.3	7.0 ± 0.9	-13.1 ± 1.4
ZnO	Lutz Madler	Hexagonal*	22.6 ± 5.1*	369.0 ± 8.5	327.6 ± 55.5	18.3 ± 0.4	-12.3 ± 2.4
ZrO ₂	US-Nano	Monoclinic*	40.1 ± 12.6*	404.9 ± 63.0	200.8 ± 10.8	-16.1 ± 0.8	-13.6 ± 2.3

*Zhang *et al.* ACS Nano 2012, 6, 4349-4368; Li *et al.* ACS Nano 2014, 8, 1771-1783.

Figure Legends:

Video S1. Time-lapse optical microscopy video to show the evolving features of pyroptosis in KUP5 cells treated with Gd_2O_3 particles. LPS-primed (1 $\mu\text{g}/\text{mL}$, 4 h) KUP5 cells were seeded into a glass bottom petri dish and exposed to 50 $\mu\text{g}/\text{mL}$ Gd_2O_3 nanoparticles. The cellular features of swelling and membrane blebbing was monitored and captured by confocal microscopy over 6 h.

Figure S1. REO nanoparticles induce pyroptosis in KUP5 cells. LPS-primed (1 $\mu\text{g}/\text{mL}$, 4 h) KUP5 cells were exposed to 12.5 $\mu\text{g}/\text{mL}$ MOx nanoparticles for 6 h. Optical microscopy images show cell swelling or membrane blebbing by REOs (except Yb_2O_3) in KUP5 cells. In contrast, ZnO nanoparticles did not induce cell swelling. The scale bar is 25 μm .

Figure S2. REO nanoparticles induce apoptotic cell death in Hepa 1-6 cells. LPS-primed (1 $\mu\text{g}/\text{mL}$, 4 h) Hepa 1-6 cells were exposed to 12.5 $\mu\text{g}/\text{mL}$ MOx nanoparticles for 18 h. Optical microscopy images show no cell swelling or membrane blebbing for REO-treated Hepa 1-6 cells. The scale bar is 25 μm .

Figure S3. Western blotting to show cleaved and activated caspases 3 and 7. The activation of these caspases was performed in KUP5 (A) and Hepa 1-6 (B) cells following their incubation with 50 $\mu\text{g}/\text{mL}$ of nanoparticle for 3 h. Immunoblotting was performed as described in Materials and Methods.

Figure S4. REOs induce NLRP3 inflammasome activation in KUP5 cells. siRNA knockdown of NLRP3 (A) and caspase-1 (B) ameliorated the REO nanoparticle-induced cell death in KUP5 cells. LPS-primed (1 $\mu\text{g}/\text{mL}$, 4 h) KUP5 cells were exposed to 200 $\mu\text{g}/\text{mL}$ MOx nanoparticles for 3 h. Cell death was determined through the use of a LDH assay. IL-1 β release in the

supernatant was quantified by ELISA (C,D). Nigericin (10 μ M) was used as a positive control. * p <0.05 compared to particle treated wild type KUP5 cells.

Figure S5. Dose-dependent IL-1 β production in response to exposure to the MOx nanoparticles in LPS-primed J774A.1, RAW 264.7 cells and BMDMs. (A-C) LPS-primed J774A.1 (1 μ g/mL, 4 h), RAW 264.7 cells (0.1 μ g/mL, 4 h) and BMDMs (1 μ g/mL, 4 h) were exposed to a wide dose range of particles (6.25-200 μ g/mL for J774A.1 and RAW 264.7 cells, and 25-200 μ g/mL for BMDMs) for 24 h. IL-1 β production in the supernatant was quantified by ELISA.

Figure S6. REO nanoparticles induce non-pyroptotic cell death in primary hepatocytes. LPS-primed (1 μ g/mL, 4 h) primary hepatocytes were exposed to 50 μ g/mL MOx nanoparticles for 24 h. (A) Cell death was determined by the MTS assay. (B) IL-1 β release in the supernatant was quantified by ELISA. Nigericin (10 μ M) was used as a positive control. Optical microscopy images show no cell swelling or membrane blebbing for REO-treated primary hepatocytes (C). The scale bar is 25 μ m. * p <0.05 compared to untreated control cells.

Figure S7. TMOs reduce intracellular GSH levels in KUP5 and Hepa 1-6 cells. KUP5 and Hepa 1-6 cells were exposed to 50 μ g/mL Co₃O₄ and ZnO nanoparticles for 24, and their intracellular GSH levels were measured by the GSH-Glo™ Glutathione Assay according to the manufacturer's instructions. * p <0.05 compared to untreated control cells.

Figure S1

KUP5 Cells

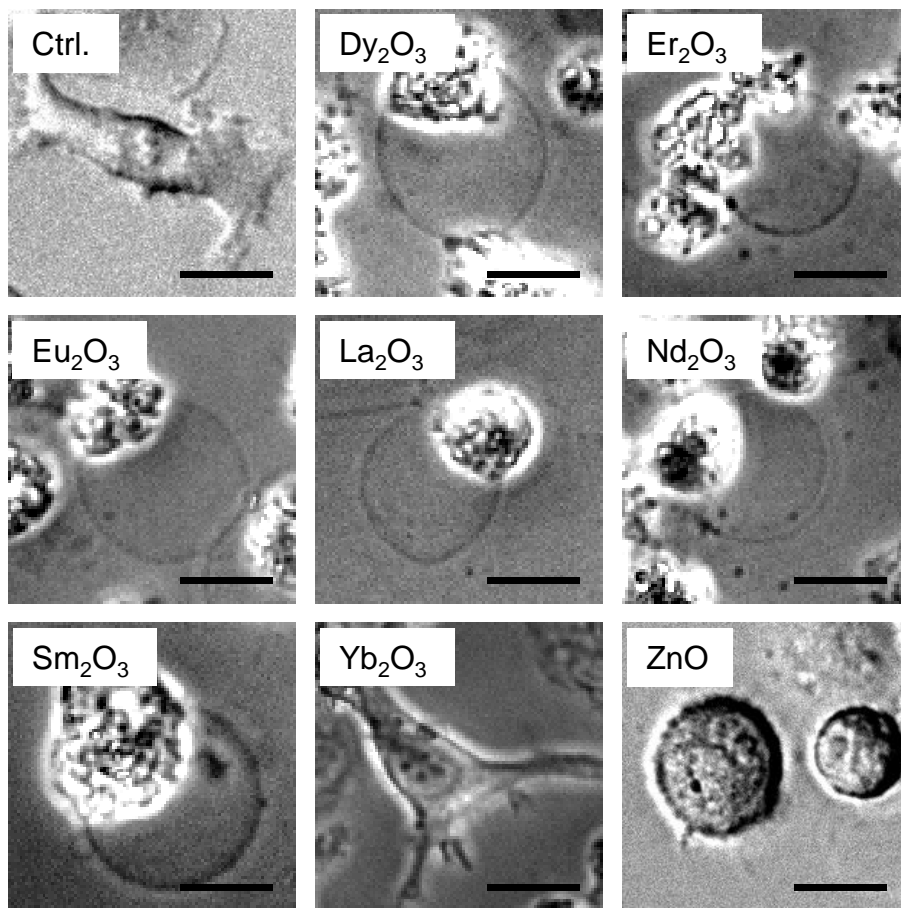


Figure S2

Hepa 1-6 Cells

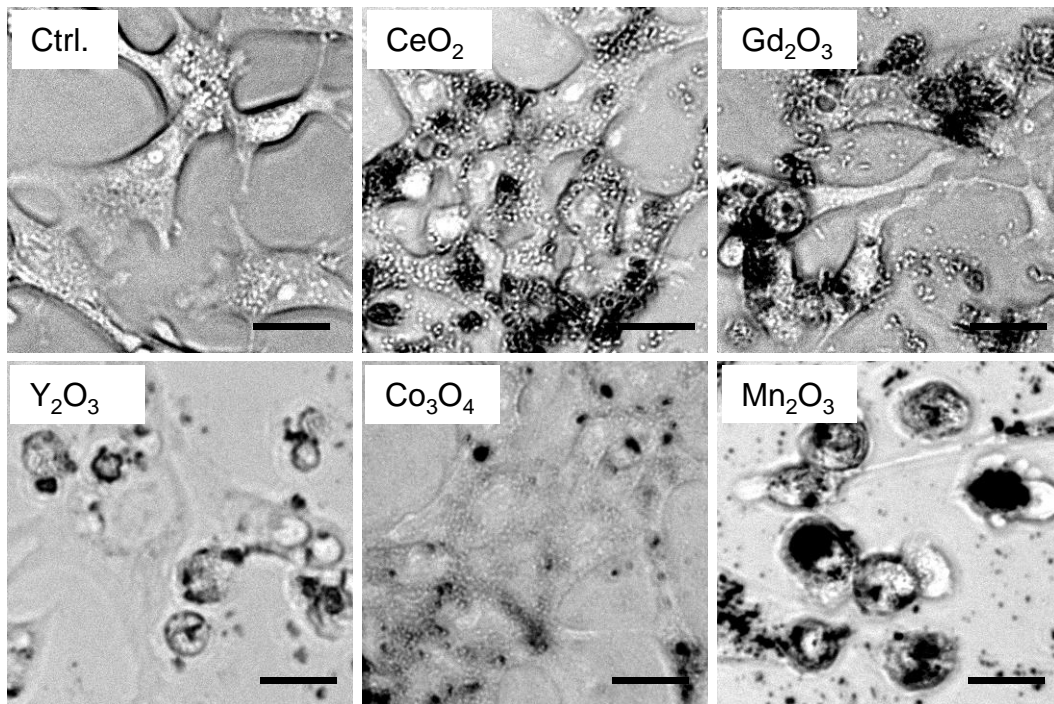
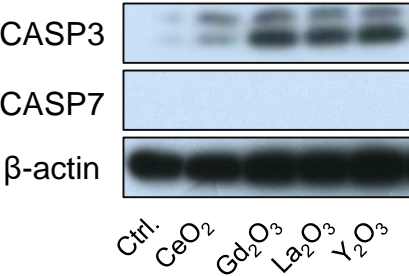


Figure S3

A KUP5 Cells



B Hepa 1-6 Cells

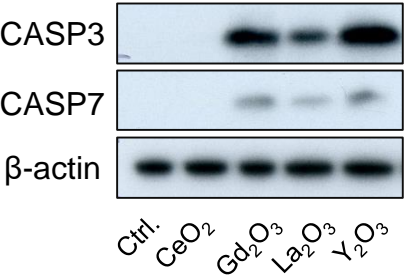
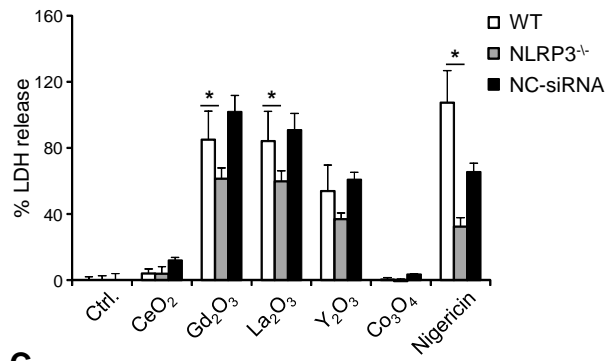


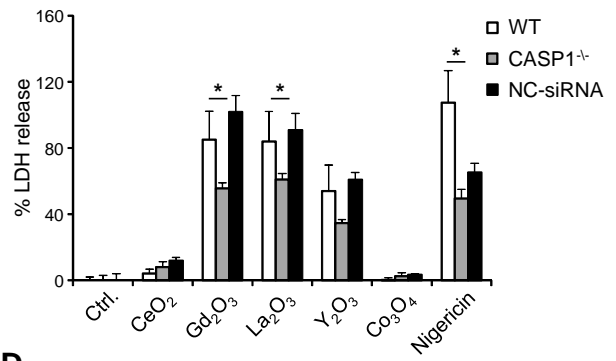
Figure S4

KUP5 Cells

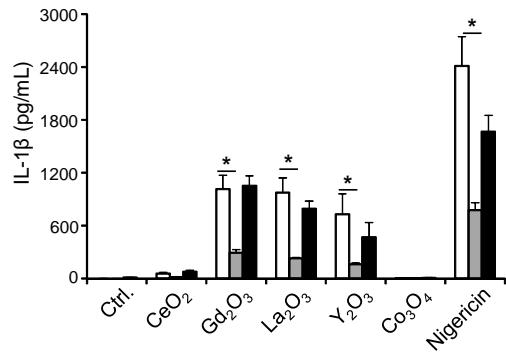
A



B



C



D

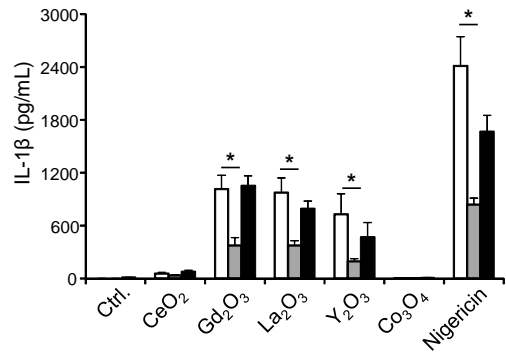
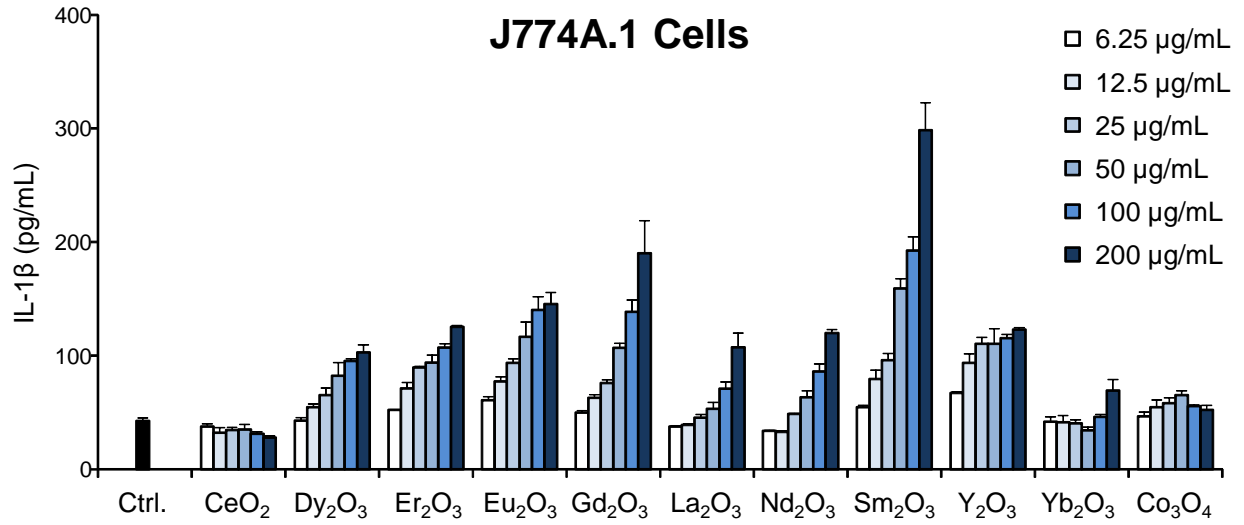
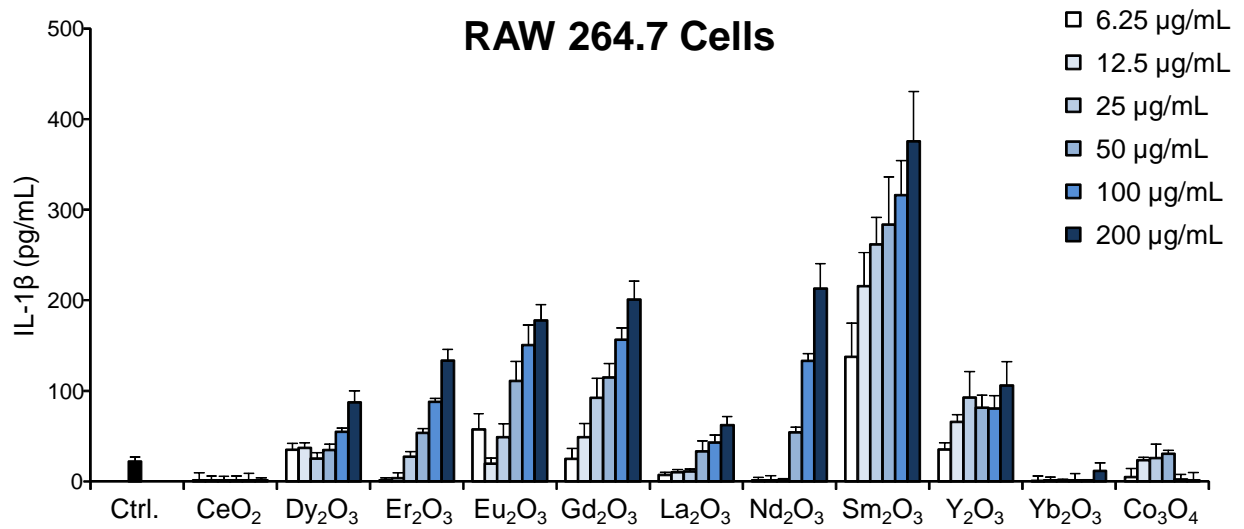


Figure S5

A



B



C

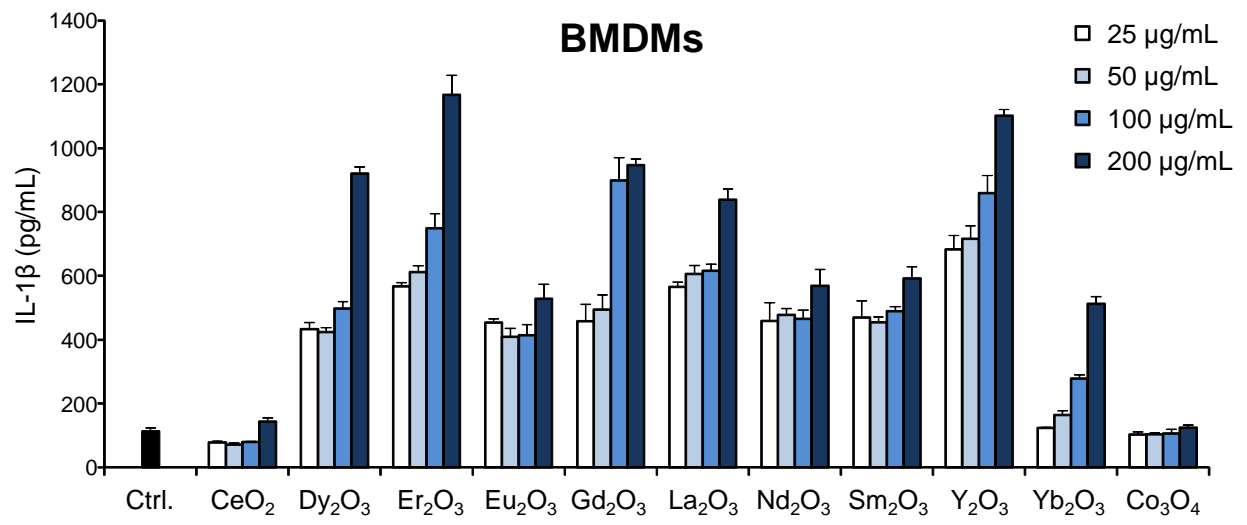


Figure S6

Primary Mouse Hepatocytes

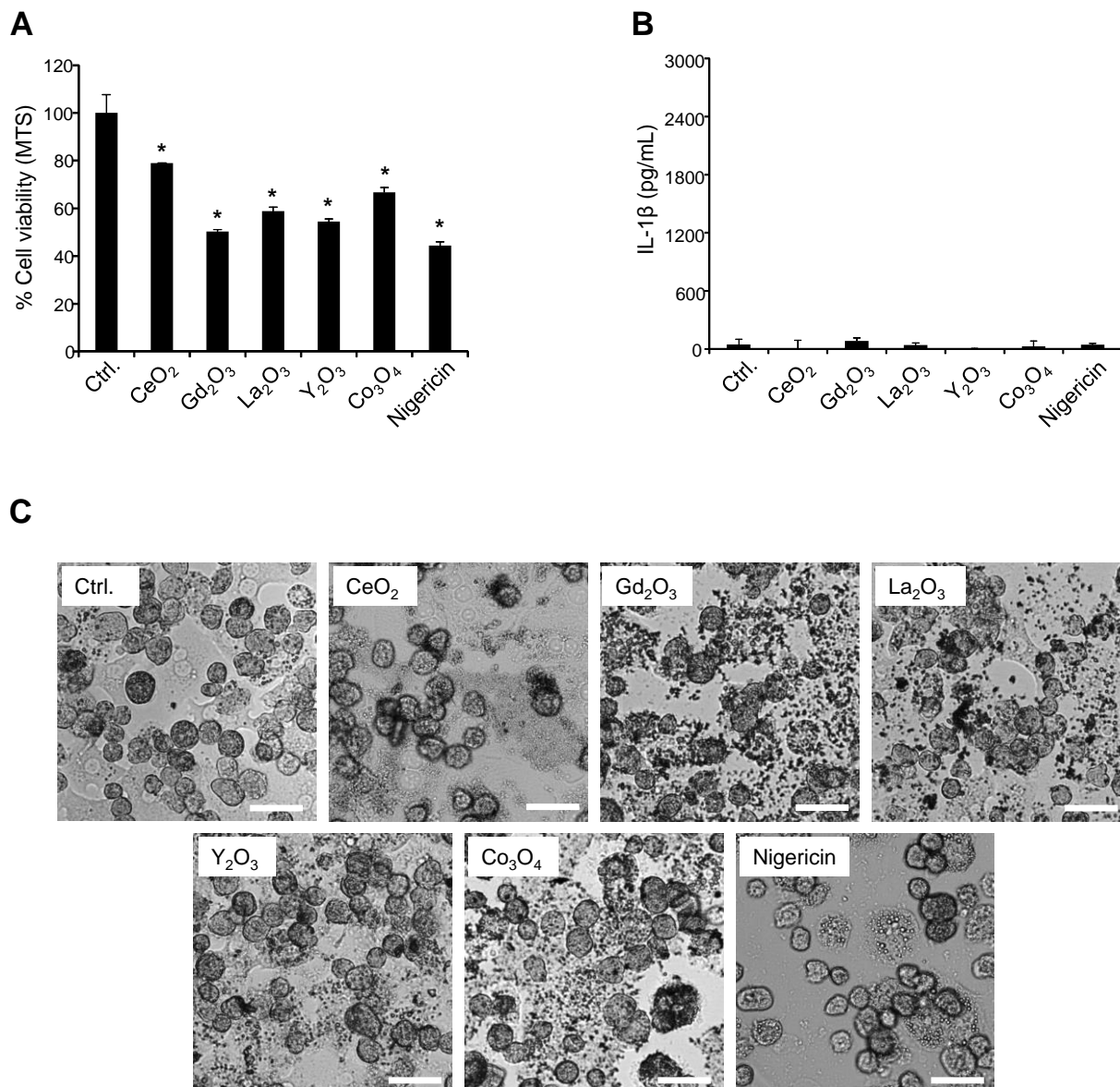


Figure S7

